

Entanglement of Group II-like atoms with fast measurement for quantum information processing

R. Stock,^{1,2,*} N. S. Babcock,¹ M. G. Raizen,³ and B. C. Sanders¹

¹*Institute for Quantum Information Science, University of Calgary, Alberta, Canada*

²*Department of Physics, University of Toronto, Toronto, Ontario, Canada*

³*Center for Nonlinear Dynamics and Department of Physics, University of Texas, Austin, Texas, USA*
(Dated: March 8, 2019)

We construct a scheme for the preparation, pairwise entanglement via exchange interaction, manipulation, and measurement of individual Group II-like neutral atoms (Yb, Sr, etc.). Group II-like atoms proffer important advantages over alkalis, including long-lived optical-transition qubits that enable fast manipulation and measurement. Our scheme provides a promising approach for producing weighted graph states, entangled resources for quantum communication and the first true violation of a Bell inequality that closes both detection and locality loopholes.

PACS numbers: 03.67.Mn, 34.50.-s, 32.80.Wr, 03.65.Ud

Introduction.— Entanglement is a vital resource for most quantum information processing (QIP) tasks, including long-distance quantum communication [1], teleportation-based quantum computation [2, 3], and one-way quantum computation (1WQC) [4]. An underappreciated but crucial aspect of QIP is the need for speed of single qubit operation, to enable applications including synchronization of quantum communication networks, measurement and feed-forward in 1WQC, and tests of local realism. For example, in 1WQC, the processor speed primarily depends on the time needed for measurement and feed-forward, whereas the entanglement operation may be slow and accomplished simultaneously before commencement of the computation. In atomic systems, single qubit fluorescence measurements are limited to microseconds due to auxiliary state lifetimes, and in alkalis single qubit rotation times are hampered by the GHz spectroscopic separations of hyperfine states. In this work, we overcome these obstacles by encoding in long-lived optical clock transitions (e.g., $^1S_0 \leftrightarrow ^3P_0$) of Group II-like neutral atoms, without sacrificing the advantages of other atomic schemes. Group II-like atoms such as Yb and Sr have long been considered for atomic clocks and much recent experimental and theoretical effort has been dedicated to this group of atoms [5, 6, 7, 8, 9, 10, 11, 12]. The recent cooling of Yb into a Bose-Einstein condensate (BEC) [9] and the ongoing study of interactions [11] make Yb an especially tantalizing candidate for atomic qubits. Our approach for entanglement and measurement of Group-II atoms offers promising techniques for the high-speed synchronization needed for quantum communication and computing, and also for the near-term violation of a Bell inequality in a single laboratory, without any assumptions about signaling, sampling, or enhancement [13, 14, 15, 16].

Significant experimental progress has been achieved towards entangling atoms in optical lattices [17], which could lead to the creation of an initial state for 1WQC. Here we take a complementary approach, considering the

entanglement of individual pairs of atoms on demand, comparable to other addressable neutral atom architectures [18]. Rather than creating a generic cluster state, we propose the creation of computation-tailored weighted graph states as a resource for 1WQC and other QIP tasks. Our technique combines efforts to prepare individual atomic qubits from a BEC [19], coherently manipulate and transport atoms [20] using optical tweezers at a “magic wavelength,” entangle atoms via an inherently robust exchange interaction [21, 22], rotate single qubits via a three-photon optical dipole transition [10], and perform fast (\sim ns) measurements via resonantly enhanced multiphoton ionization (REMPI). A “loop-hole free” Bell inequality test imposes stringent requirements on detector separation and efficiency, and therefore presents an enticing test-bed for fast measurements with applications to QIP. Here we study the limits of fast measurement for encoding in the optical clock states of Yb and Sr, which can be resolved spectroscopically and measured on a \sim 10ns timescale, thereby admitting space-like separation over a few meters. We show that such Bell tests in a single laboratory should be feasible via a detailed theoretical analysis accompanied by comprehensive numerical simulations of realistic experimental conditions.

Qubit preparation and transport.— Optical clock transitions in alkaline-earth and Group II-like atoms are appealing candidates for encoding qubits due to extremely low decoherence rates, permitting quantum information to be stored for long times, even during transport over several meters. Single atoms have been experimentally isolated and transported in optical dipole traps [20], and increasingly sophisticated atom-trapping methods continue to be developed [19]. By trapping at a “magic wavelength” [7, 8], the light shift potential is made effectively state-independent. Dephasing effects due to field fluctuations are thereby suppressed.

Entangling Operation.— We devise a universal entangling operation for bosons, analogous to the recently proposed fermionic spin-exchange gate [21]. This gate

is based on the exchange interaction recently demonstrated for bosonic Rb atoms in a double-well optical lattice [22]. Because of inherent symmetrization requirements, gates based on this exchange interaction offer a natural resistance to errors and greater flexibility for encoding atoms, thereby enabling an entangling operation even for atoms with interaction strengths that are state-independent (e.g., Rb [22]) or partially unknown, as is the case for most Group II-like atoms (e.g., Yb [11]).

The entangling operation is achieved by temporarily bringing together a pair of atomic qubits via mobile optical tweezers. Unlike state-dependent optical traps wherein atoms are trivially separated into opposite wells after interaction, we have state-independent traps in which the dynamics of the system generally determine the likelihood of a successful separation. However, under adiabatic conditions the atoms definitely end up in opposite wells. We assume a strong confinement to 1D by higher order Hermite Gaussian beams according to [19]. All the essential physics is captured in the 1D model we employ here, although performance could conceivably be enhanced by exploiting multi-dimensional effects such as trap-induced resonances [23].

The Hamiltonian for two atoms a and b with internal structure ($|i\rangle_a, |j\rangle_b \in \{|0\rangle, |1\rangle\}$) trapped in two wells is given by

$$H = \sum_{i,j=0,1} [H_a + H_b + 2a_{ij}\hbar\omega_\perp\delta(x_a - x_b)] \otimes |ij\rangle\langle ij| \quad (1)$$

for $H_{a,b} \equiv p_{a,b}^2/2m + V(x_{a,b} - d/2) + V(x_{a,b} + d/2)$, with $x_{a,b}$ and $p_{a,b}$ the position and momentum of atom a or b. The tweezer potential $V(x) = -V_o \exp(-x^2/2\sigma^2)$ describes a Gaussian trap of depth V_o and variance σ^2 . Traps are separated by a distance d , ω_\perp is the harmonic oscillation frequency of the transverse confinement [24], and a_{ij} is the state-dependent scattering length for the two-qubit states $|ij\rangle \equiv |i\rangle_a \otimes |j\rangle_b$. We numerically solve the Hamiltonian dynamics of individual qubit states using a split-operator method. Two-atom energy spectra are plotted as a function of well separation (Fig. 1) for different interaction strengths.

Due to symmetrization requirements, not all combinations of vibrational and qubit states are allowed. For example, a pair of composite bosons cannot share the ground state if the qubits are in the antisymmetric state $|\Psi^-\rangle$, defining $|\Psi^\pm\rangle \equiv (|01\rangle \pm |10\rangle)/\sqrt{2}$. As in the fermionic case [21], it is possible to exploit these symmetrization requirements in order to produce a two-qubit entangling operation for bosonic atoms (see [25] for details). Consider a pair of identical bosons, one localized in the left trap ($|\psi^L\rangle$) and carrying a qubit in the state $|\varphi^\alpha\rangle = \alpha|0\rangle + \beta|1\rangle$, the other in the right trap ($|\psi^R\rangle$) and carrying a qubit in the state $|\varphi^\mu\rangle = \mu|0\rangle + \nu|1\rangle$. The initial symmetrized wavefunction (as a tensor product of vibrational and qubit states) is then $|\psi_i\rangle = (|\psi^L\psi^R\rangle \otimes |\varphi^\alpha\varphi^\mu\rangle + |\psi^R\psi^L\rangle \otimes |\varphi^\mu\varphi^\alpha\rangle)/\sqrt{2}$.

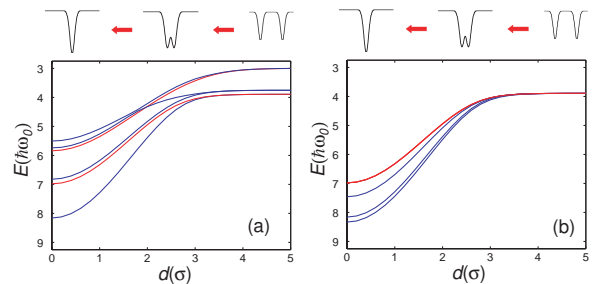


FIG. 1: Adiabatic energy levels as a function of well separation. (a) Lowest six energy levels for $a_{ij} = 0.1\sigma$. Energy levels corresponding to symmetric external eigenstates are shown in blue, antisymmetric in red. Energies are measured in units of $\hbar\omega_o$, where ω_o is the harmonic oscillation frequency of one atom in a single well. (b) Lowest two levels for different scattering lengths. The blue energy curves (from bottom to top) correspond to $a_{ij} = 0$, $a_{ij} = 0.1\sigma$, and $a_{ij} = \sigma$ and asymptote to the red curves for infinite a_{ij} . The antisymmetric eigenstates are not affected by the interaction and the red curve does not shift for different a_{ij} . (Colour online.)

As the wells are brought together and separated adiabatically, the energies evolve as shown in Fig. 1, and each two-qubit state $|00\rangle, |11\rangle, |\Psi^\pm\rangle$ acquires a phase $\phi_{00}, \phi_{11}, \phi_\pm$, depending on its respective energy curve. Adiabaticity can be fulfilled even for negative scattering lengths, since transitions between vibrational states of different symmetry or parity are suppressed. For constant tweezer speed v , we derive the approximate adiabaticity criterion to be $v \ll \sigma\hbar\omega_{ab}^2/V_o$ [25], with $\hbar\omega_{ab}$ the energy difference between coupled states. Time-dependent numerical simulations confirm the validity of this criterion over a wide range of values of V_o and a_{ij} . The final state after an adiabatic change of separation is

$$|\psi_f\rangle = |\psi^-\rangle \otimes \left(\frac{\alpha\nu - \beta\mu}{\sqrt{2}} e^{-i\phi_-} |\Psi^-\rangle \right) + |\psi^+\rangle \otimes \left(\alpha\mu e^{-i\phi_{00}} |00\rangle + \beta\nu e^{-i\phi_{11}} |11\rangle + \frac{\alpha\nu + \beta\mu}{\sqrt{2}} e^{-i\phi_+} |\Psi^+\rangle \right), \quad (2)$$

using $|\psi^\pm\rangle \equiv (|\psi^L\psi^R\rangle \pm |\psi^R\psi^L\rangle)/\sqrt{2}$.

Evidently this process corresponds to a tensor product of the identity acting on the vibrational state and a unitary U acting on the qubit state. Thus, the internal qubit evolution simplifies to

$$U = e^{-i\phi_{00}} |00\rangle\langle 00| + \frac{e^{-i\phi_+} + e^{-i\phi_-}}{2} (|01\rangle\langle 01| + |10\rangle\langle 10|) + \frac{e^{-i\phi_+} - e^{-i\phi_-}}{2} (|01\rangle\langle 10| + |10\rangle\langle 01|) + e^{-i\phi_{11}} |11\rangle\langle 11|. \quad (3)$$

As in [26], a controlled-phase gate can be obtained even if $\phi_+ \neq \phi_-$ by sandwiching a single-qubit phase gate between a pair of U operations. That is, $G \equiv U[S(\pi) \otimes S(0)]U$ for $S(\theta) = \exp(i\theta|1\rangle\langle 1|)$. Thus defined, G is locally equivalent to $\exp(i\gamma|11\rangle\langle 11|)$ if

$$\phi_{00} + \phi_{11} - \phi_+ - \phi_- = (2n \pm \frac{1}{2})\gamma, \quad \forall n \in \mathbb{Z}. \quad (4)$$

As shown in Eq. (2), the phases critical to this entangling operation are acquired in a non-separable basis. This leads to the inherent robustness observed in initial experiments [22]. In standard schemes, the important non-separable phase is usually acquired due to the internal state dependence of the interaction strengths a_{ij} . In the case of this exchange symmetry-based gate, however, there always is an energy gap between symmetric and antisymmetric curves. The singlet state $|\Psi^-\rangle$ therefore acquires a phase different from the triplet states even if interaction strengths are state-independent (except as $a_{ij} \rightarrow \pm\infty$). This substantial phase difference enables the exchange gate to operate faster than standard collisional gates that rely on the difference in a_{ij} . Furthermore, this gate works over a large range of scattering lengths (see Fig 1b), which is especially important when designing experiments for atomic species with any unknown scattering lengths (e.g., Yb or Sr). Current studies of Yb interactions [11] already promise a wide applicability of this entanglement gate for different isotopes. (For ^{168}Yb , $a_{00} \approx 13$ nm and for ^{174}Yb , $a_{00} \approx 5.6$ nm. Other interaction strengths, a_{01} and a_{11} , are not yet known.)

Single qubit rotation and measurement.— Recent attempts to cool and trap neutral Yb and Sr have been very successful, and we therefore consider them primarily. Optical clock states in even isotopes of Yb and Sr have extremely low decoherence rates, due to the fact that electric dipole one- and two-photon transitions between $^1\text{S}_0$ and $^3\text{P}_0$ states are dipole- and parity-forbidden, respectively (see Figs.2(a) and 3(a) for energy levels and transition wavelengths). While affording long lifetimes, these selection rules also present a significant challenge to fast coherent manipulation and measurement of qubits. To overcome this challenge, we employ a coherent, three-photon transition to perform single qubit operations, utilizing the excited $^3\text{S}_1$ and $^3\text{P}_1$ states [10]. The three transitions $^1\text{S}_0 \rightarrow ^3\text{P}_1$, $^3\text{P}_1 \rightarrow ^3\text{S}_1$, and $^3\text{S}_1 \rightarrow ^3\text{P}_0$ are electric-dipole allowed (see [5, 6] for transition matrix elements). Because three beams can always be arranged in a plane such that the transferred recoil cancels, this three-photon transition has the added benefit of being recoil-free [10], thereby reducing decoherence effects due to heating. For Sr, the need for three lasers may be reduced to two, as explained below.

We model this three-photon transition by a master equation using the Liouvillian matrix given in [10]. Its fidelity is limited by the short-lived intermediate $^3\text{S}_1$ state, which decays primarily to the $^3\text{P}_1$ state. The fast coherent rotation of qubits is followed by the fast readout of the $^3\text{P}_0$ state via REMPI on a nanosecond or even picosecond timescale. Re-using the $^3\text{S}_1$ excited state, photoionization can then be accomplished in a two-step process. An on-resonant $^3\text{P}_0$ to $^3\text{S}_1$ transition is followed by a final ionization step at $\lambda < 563$ nm for Yb and $\lambda < 592$ nm for Sr. The main errors in this read-out scheme are due

to population in the $^3\text{P}_1$ to $^3\text{S}_1$ states. During readout, any population in $^3\text{P}_0$ and $^3\text{S}_1$ will be counted as logical $|1\rangle$ (ionized). Population in $^1\text{S}_0$ and $^3\text{P}_1$ will be counted as logical $|0\rangle$ (not ionized).

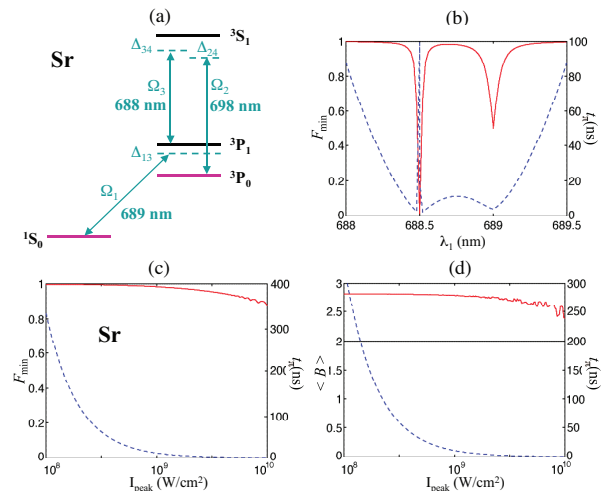


FIG. 2: (a) Energy levels of Sr and three-photon transition for manipulation of the qubit encoded in $^1\text{S}_0$ and $^3\text{P}_0$. (b) Minimum fidelity F_{min} of single qubit operation in Sr (solid red line) and timescale for π pulse (dashed blue line) as a function of λ_1 ($= \lambda_3$) using a peak laser pulse intensity of 10^9 W/cm 2 . (c) Minimum fidelity F_{min} of single qubit operation (solid red line) and timescale for π pulse (dashed blue line) as a function of laser intensity. Detuning is fixed to $\lambda_1 = 688.7$ nm. (d) Resulting expectation value of the Bell operator $\langle B \rangle$ and threshold for a local hidden variable model (solid black line).

The case of Sr is particularly interesting: the transitions $^1\text{S}_0 \rightarrow ^3\text{P}_1$ and $^3\text{P}_1 \rightarrow ^3\text{S}_1$ are close in energy difference (689 nm and 688 nm, respectively) and a resonant two-photon transition $^1\text{S}_0 \rightarrow ^3\text{S}_1$ utilizing a single laser is possible. This reduces the laser requirement from three to two. Figure 2(b) show fidelities for qubit rotation for wavelengths in the range 688 nm to 689.5 nm. The time for a π -rotation is minimized by tuning to 688.7 nm. Figure 2(c) shows the fidelity and timescales for a π -rotation as a function of laser powers. For fairly realistic mode-locked laser powers, 10^9 W/cm 2 (roughly 1 kW pulse peak power focused onto $100\mu\text{m}^2$), rotations within a few nanoseconds are possible with $> 90\%$ fidelity. Higher fidelities of 99.99% can be reached for the same detuning using lower laser powers of 10^6 W/cm 2 .

Tests of local realism.— We show the efficacy of our fast measurement scheme by applying it to a test of local realism. This is expressed in the usual Clauser-Horne-Shimony-Holt (CHSH) form [13],

$$\langle B \rangle = \langle QS \rangle + \langle RS \rangle + \langle RT \rangle - \langle QT \rangle \leq 2, \quad (5)$$

for local realistic theories, whereas Tsirelson's quantum upper bound is $2\sqrt{2}$. The quantum bound is saturated for measurements $Q = Z$, $R = X$, $S = X + Z$, $T =$

$X - Z$, with X , Y , and Z the Pauli operators. These measurements are obtained via basis rotations of the form $Q = U_Q^\dagger Z U_Q$. The corresponding rotations are $U_Q = \mathbb{1}$, $U_R = R(\pi/2)$, $U_S = R(3\pi/4)$, and $U_T = R(\pi/4)$, where $R(\theta) = \exp(-i\theta Y/2)$.

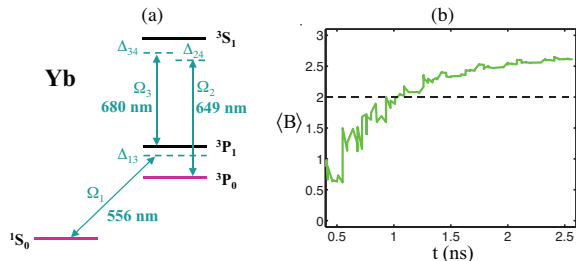


FIG. 3: (a) Energy levels of Yb and three-photon transition for manipulation of the qubit encoded in 1S_0 and 3P_0 . (b) Expectation value of the Bell operator for imperfect single-qubit rotations in Yb as a function of timescale of the measurement for $I_{\text{peak}} = 10^9 \text{ W/cm}^2$.

Inequality (5) is tested by first preparing an entangled Bell state via a controlled phase gate as discussed above, then separating the atoms by several meters. At this distance, synchronous measurements on a nanosecond timescale are required to ensure space-like separation. Within this time window, the measurement basis is chosen randomly, qubits are rotated to reflect the choice of measurement basis, and qubit states are measured in the computational basis using REMPI. Fast random basis selection can be accomplished by using a light-emitting diode as in [15]. The time necessary for this random basis selection can be minimized (e.g., by using shorter signal paths and custom-built EOMs) to ensure basis selection times of $< 10\text{ns}$. Rotation of the measurement basis is achieved via a coherent coupling of the qubit states via three-photon Raman transitions. The presence of the ion (i.e., the freed electron) will be detected via a high-bias proportional detector.

As in a typical single channel experiment [16], the measurement outcome can be only “ion” $\equiv |1\rangle$ or “no ion” $\equiv |0\rangle$. The experiment may be repeated with a repetition rate on the order of seconds to allow for the entangling operation and transport of atoms over a few meters. No data are discarded, and no assumptions are made about “fair sampling” [13] or “enhancement” [14]. Loss of an atom will result in a “no ion” $\equiv |0\rangle$ count, which reduces the degree of Bell inequality violation but does not open any loopholes. High transport and detector efficiencies are therefore necessary to ensure that a violation occurs. A detailed calculation of the CHSH-type Bell inequality violation [13], including errors in rotation and ionization readout, is shown in Fig. 2d for Sr and Fig. 3b for Yb. To achieve an average value of the Bell-operator larger than 2, as required for a violation, measurements on a time scale of a few ns (including signal processing

times) should be possible with either atomic species.

Conclusions.— We propose schemes for fast recoil-free manipulation and measurement of qubits in Sr and Yb, and discuss an entangling operation for identical atoms in optical tweezers based on exchange interaction first discussed for fermions in [21]. We furthermore show that it is possible to simultaneously close both space-like separation and detection loopholes for Group II-like atomic qubits separated on only a laboratory scale. This lays the groundwork for future exploration of measurement-based computation and synchronization of small-scale quantum computers. Finally, our work identifies major challenges and provides concrete guidelines for experiments utilizing bosonic Yb and Sr for quantum information processing applications.

We thank P. Julienne and A. Derevianko for helpful discussions on Yb and Sr, W. Ketterle for discussions on long-distance transport of atoms, D. Hayes and I. Deutsch for discussions on entangling atoms via exchange interactions, and K. Resch and G. Weihs for discussions on Bell inequalities. This work was supported by NSERC, AIF, CIFAR, iCORE, MITACS, NSF, and The Welch Foundation.

* Electronic address: restock@physics.utoronto.ca

- [1] H.-J. Briegel, W. Dür, J. I. Cirac, and P. Zoller, *Phys. Rev. Lett.* **81**, 5932 (1998).
- [2] D. Gottesman and I. L. Chuang, *Nature* **402**, 390 (1999).
- [3] E. Knill, R. Laflamme, and G. J. Milburn, *Nature* **409**, 46 (2001).
- [4] R. Raussendorf and H.-J. Briegel, *Phys. Rev. Lett.* **86**, 5188 (2001).
- [5] H. G. C. Werij, C. H. Greene, C. E. Theodosiou, and A. Gallagher, *Phys. Rev. A* **46**, 1248 (1992).
- [6] S. G. Porsev, Y. G. Rakhlina, and M. G. Kozlov, *Phys. Rev. A* **60**, 2781 (1999).
- [7] M. Takamoto and H. Katori, *Phys. Rev. Lett.* **91**, 223001 (2003).
- [8] S. G. Porsev, A. Derevianko, and E. N. Fortson, *Phys. Rev. A* **69**, 021403(R) (2004).
- [9] Y. Takasu *et al.*, *Phys. Rev. Lett.* **91**, 040404 (2003).
- [10] T. Hong, C. Cramer, W. Nagourney, and E. N. Fortson, *Phys. Rev. Lett.* **94**, 050801 (2005).
- [11] M. Kitagawa *et al.*, arXiv:0708.0752 (2007).
- [12] Z. W. Barber *et al.*, *Phys. Rev. Lett.* **96**, 083002 (2006).
- [13] J. F. Clauser, M. A. Horne, A. Shimony, and R. A. Holt, *Phys. Rev. Lett.* **23**, 880 (1969).
- [14] J. F. Clauser and M. A. Horne, *Phys. Rev. D* **10**, 526 (1974).
- [15] G. Weihs *et al.*, *Phys. Rev. Lett.* **81**, 5039 (1998).
- [16] M. A. Rowe, D. Kielpinski, V. Meyer, C. A. Sackett, W. M. Itano, C. Monroe, and J. Wineland, *Nature* **409**, 791 (2001).
- [17] For a review see *Nature Insight*, *Nature* **416**, 205 (2002).
- [18] R. Dumke *et al.*, *Phys. Rev. Lett.* **89**, 097903 (2002), K. Eckert *et al.*, *Phys. Rev. A* **66**, 042317 (2002), R. Folman *et al.*, *Adv. At. Mol. Opt. Phys.* **48**, 263-356 (2002).

- [19] T. P. Meyrath *et al.*, Opt. Express **13**, 2843 (2005), A. M. Dudarev, M. G. Raizen and Q. Niu, Phys. Rev. Lett. **98**, 063001 (2007).
- [20] J. Beugnon *et al.*, arXiv:0705.0312 (2007).
- [21] D. Hayes, P. S. Julienne, and I. H. Deutsch, Phys. Rev. Lett. **98**, 070501 (2007).
- [22] M. Anderlini *et al.*, Nature (London) **448**, 452 (2007).
- [23] R. Stock, I. H. Deutsch, and E. L. Bolda, Phys. Rev. Lett. **91**, 183201 (2003).
- [24] T. Calarco *et al.*, Phys. Rev. A **61**, 022304 (2000).
- [25] N. S. Babcock, R. Stock, M. G. Raizen and B. C. Sanders, submitted to Can. J. Phys.
- [26] D. Loss and D. P. DiVincenzo, Phys. Rev. A **57**, 120 (1998).